Industry Science and Engineering Vol. 3 No. 9, 2026

Research on Cooperative Motion of Mobile Robots Based on Nonlinear Model Predictive Control

Tingting Zhang
College of Intelligent Manufacturing, Chongqing Industry & Trade Polytechnic, Chongqing, China

Abstract: For mobile robots in collaborative tasks, the coordinated control of mobile base and manipulator suffers from decoupling difficulties. Meanwhile, motion planning in high-dimensional spaces requires considerable computation. This paper proposes a coordinated motion control scheme for mobile manipulators based on nonlinear model predictive control (NMPC), which enables stable coordinated motion between the mobile base and manipulator. The complete kinematic model of the mobile robot is established, and an NMPC-based coordinated controller is designed. A simulation model is built in Simulink and CoppeliaSim. The optimal control trajectory is calculated by minimizing the given objective function, and the proposed scheme is verified in simulation environments. The results show that the mobile base and manipulator can work coordinately. When the end-effector moves at 0.5 m/s, 1.0 m/s and 1.5 m/s, its average tracking error is between 4.63 cm and 14.87 cm, and the average tracking error of the mobile base ranges from 4.18 cm to 12.53 cm.

Keywords: Mobile Robot; Mobile Manipulator Coordination; Trajectory Tracking; NMPC

1. Introduction

Mobile robots are widely used in industrial production, logistics handling, factory inspection and agricultural applications. For such robots, both the mobile base and the manipulator end-effector need to follow predefined trajectories. Generally, the end-effector is required to track the task trajectory accurately, while the mobile platform moves along a safe path. Therefore, mobile robots are subject to dual constraints: path tracking of the base and trajectory tracking of the manipulator end-effector during continuous operation. If the two parts work in coordination, the mobile base can support the manipulator to operate over a larger workspace with higher efficiency. Under such requirements, automatic coordinated control of mobile robots is of great significance.

Compared with the separate control of the mobile base and manipulator, the coordinated motion control of mobile manipulators needs to consider their motion coupling, which leads to higher system complexity. For system modeling, existing studies generally follow two approaches: integrated modeling and separate modeling. Integrated modeling treats the mobile base and manipulator as a unified system and can fully describe their kinematic or dynamic coupling [1] By contrast, separate modeling [2] establishes mathematical models for the mobile base and manipulator individually, and achieves motion coordination through a coordination mechanism. Mobile manipulator systems feature multiple degrees of freedom, nonlinearity and complicated coupling. It is difficult to build an accurate integrated dynamic model, and the corresponding computation is heavy. For this reason, some studies simplify the coupling relationship and construct control models at the kinematic or dynamic level separately to reduce the computational burden of model solving [3].

In terms of motion planning, mobile manipulators must satisfy the motion constraints of the mobile base and the task requirements of the end-effector simultaneously. Existing planning methods can be classified into integrated planning [4] and hierarchical planning [5,6]. Integrated planning incorporates the motion variables of the mobile base and manipulator into a unified planning framework. It can take full account of system motion constraints and coordination relations, yet the computational complexity rises as the number of system degrees of freedom increases. Hierarchical planning decomposes the planning tasks of the base and manipulator to reduce the complexity of a single planning problem. Nevertheless, extra work is required to handle the coordination between different planning

layers [7].

In the field of coordinated motion control, model predictive control (MPC) can handle multivariable coupling and system constraints within a unified optimization framework. For this reason, it has been gradually adopted for the integrated coordinated control of mobile manipulators [8]. For mobile manipulators subject to nonholonomic constraints, some existing works combine MPC with control barrier functions to achieve safe trajectory tracking under multiple constraints [9,10]. Besides, relevant studies have proposed task-priority coordination methods based on whole-body model predictive control. Such methods improve trajectory tracking performance and manipulator manipulability while satisfying the nonholonomic kinematic constraints of the base [11] Reference [12] further realizes coordinated motion control for multi-task scenarios by jointly optimizing the motion variables of the mobile base and manipulator.

This paper investigates a coordinated motion control method for autonomously operating mobile manipulators. Different from the traditional strategy of solving the inverse kinematics of redundant manipulators, an NMPC-based coordination framework for the mobile base and manipulator is proposed. The optimal control trajectory is obtained by minimizing a predefined objective function. Meanwhile, the controller generates velocity commands for the mobile platform to track the reference path. This arrangement ensures that the end-effector follows the desired task trajectory, while the mobile platform moves along its pre-planned path. The platform velocity along its path is fully determined by the manipulator state. Simulations are carried out in the virtual environment built on the CoppeliaSim physics simulator. Several typical task scenarios are tested, and satisfactory tracking performance is achieved.

2. Coordinated Motion Control of the Mobile Manipulator

2.1 Problem Formulation

As shown in Figure 1, the coordinated motion control problem studied in this work is described as follows. Given the reference trajectory of the manipulator end-effector and the reference path of the mobile platform, the motions of the manipulator and mobile platform are coordinated. The end-effector is required to move along its reference trajectory at a preset speed. Meanwhile, the travelling speed of the mobile platform is adjusted dynamically according to the motion state of the manipulator to realize coordinated motion. The trajectory tracking error of the end-effector and the path tracking error of the mobile platform should be kept within acceptable bounds.

To achieve the above control objectives, this paper constructs a mobile base-manipulator coordinated control framework consisting of a motion planning module and a coordinated control module. The motion planning module generates the end-effector trajectory and the mobile platform path separately and supplies reference signals to the coordinated controller. The coordinated control module accounts for the kinematic coupling between the mobile platform and manipulator, establishes the integrated kinematic model of the mobile manipulator, and designs the coordinated controller using the NMPC method. By jointly optimizing the motion variables of the mobile platform and manipulator, accurate tracking of the reference trajectory by the end-effector and stable tracking of the reference path by the mobile platform are realized. The longitudinal and lateral motion control of the mobile platform is integrated into this coordinated framework for the coordinated optimization of the whole system.

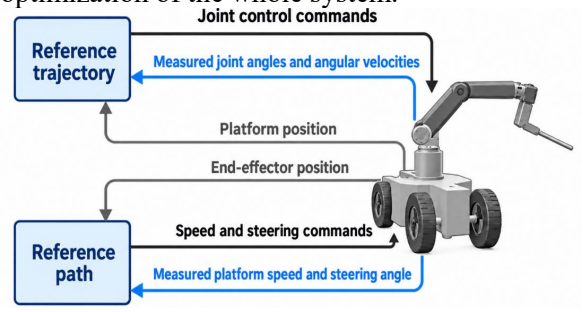


Figure 1. Schematic of Coordinated Control for the Mobile Robot

2.2 Overall Kinematic Model of the Mobile Manipulator

The position of the manipulator end-effector in the global coordinate frame can be derived from the kinematic models of the mobile base and the manipulator, so as to obtain the overall kinematic model of the robot. Figure 2 shows the schematic diagram of the robot model.

The coordinates of the mobile base in the global coordinate frame (denoted by w) are defined as

$[X_m, Y_m, \varphi]$. Accordingly, the pose matrix of the mobile base under the global coordinate frame is:

$$ {}^{w}T_m = \begin{bmatrix} \cos\varphi & -\sin\varphi & 0 & X_m \\ \sin\varphi & \cos\varphi & 0 & Y_m \\ 0 & 0 & 1 & 0 \\ 0 & 0 & 0 & 1 \end{bmatrix} \tag{1} $$

The transformation matrix of the manipulator base relative to the center of the mobile platform's rear axle is expressed as:

$$ {}^{m}T_{ef} = \begin{bmatrix} 1 & 0 & 0 & 0 \\ 0 & 1 & 0 & d_l \\ 0 & 0 & 1 & d_h \\ 0 & 0 & 0 & 1 \end{bmatrix} \tag{2} $$

where d_l and d_h represent half of the wheelbase and half of the base height, respectively.

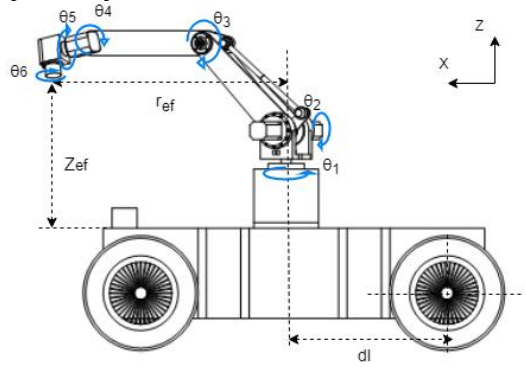


Figure 2. Simplified Robot Model

Then the transformation matrix of the manipulator end-effector with respect to the global coordinate frame is:

$$ {}^{w}T_{ef} = {}^{w}T_m \, {}^{m}T_{ef} \, {}^{0}T_6 $$

$$ = \begin{bmatrix} r_{11}\cos\varphi - r_{21}\sin\varphi & r_{12}\cos\varphi - r_{22}\sin\varphi & r_{13}\cos\varphi - r_{23}\sin\varphi & X_m + p_x\cos\varphi - d_l\sin\varphi - p_y\sin\varphi \\ r_{21}\cos\varphi + r_{11}\sin\varphi & r_{22}\cos\varphi + r_{12}\sin\varphi & r_{23}\cos\varphi + r_{13}\sin\varphi & Y_m + d_l\cos\varphi + p_y\cos\varphi + p_x\sin\varphi \\ r_{31} & r_{32} & r_{33} & d_h + p_z \\ 0 & 0 & 0 & 1 \end{bmatrix} \tag{3} $$

The position coordinates $[p_x, p_y, p_z]$ of the manipulator end-effector with respect to the manipulator base are expressed as:

$$ \begin{aligned} p_z &= d_4 s_1 + a_4 c_{23} c_1 + a_3 c_1 c_2 + d_5 s_{234} c_1 + d_6 \left[c_{234} c_1 s_5 - c_5 s_1 \right] \\ p_y &= d_4 c_1 + a_4 c_{23} s_1 + a_3 c_2 s_1 + d_5 s_{234} s_1 + d_6 \left[c_1 c_5 + c_{234} s_1 s_5 \right] \\ p_z &= d_1 - d_5 c_{234} + a_4 s_{23} + a_3 s_2 + d_6 s_5 s_{234} \end{aligned} \tag{4} $$

Therefore, given the position coordinates of the mobile chassis, the yaw angle, and the position of the manipulator relative to its base, the end-effector position in the global coordinate frame can be derived as:

$$ P_{ef} = \begin{bmatrix} X_m - d_l \sin\varphi + p_x \cos\varphi - p_y \sin\varphi \\ Y_m + d_l \cos\varphi + p_x \sin\varphi + p_y \cos\varphi \\ p_z + d_h \end{bmatrix} \tag{5} $$

Differentiating Eq. (5), the velocity matrix of the end-effector can be obtained as:

$$ v_{ef} = \begin{bmatrix} \dot{X}_m - d_l \cos(\varphi)\dot{\varphi} + \dot{p}_x \cos\varphi - p_x \sin(\varphi)\dot{\varphi} - \dot{p}_y \sin\varphi - p_y \cos(\varphi)\dot{\varphi} \\ \dot{Y}_m - d_l \sin(\varphi)\dot{\varphi} + \dot{p}_x \sin\varphi + p_x \cos(\varphi)\dot{\varphi} + \dot{p}_y \cos\varphi - p_y \sin(\varphi)\dot{\varphi} \\ \dot{p}_z \end{bmatrix} \tag{6} $$

3 Design of NMPC-Based Mobile Manipulator Coordination Control

3.1 Discretization of the Prediction Model

For notation convenience, let $q = [\theta_1, \theta_2, \cdots \theta_6]$ and $\dot{q} = [\dot{\theta}_1, \dot{\theta}_2, \cdots \dot{\theta}_6]$ The robot state vector is defined as $X = [x, y, \varphi, v, \delta, q, \dot{q}]$, which contains 17 state variables in total: the first 5 describe the chassis states, and the remaining 12 describe the manipulator's joint configuration and velocities. The control vector consists of the chassis velocity, steering angle, and manipulator joint velocities, $u = [v_u, \delta_u, \dot{\theta}_{u1}, \dot{\theta}_{u2}, \dot{\theta}_{u3}, \dot{\theta}_{u4}, \dot{\theta}_{u5}, \dot{\theta}_{u6}]$

Given the large number of state variables, discretization is performed individually for each state.

The fourth-order Runge–Kutta method is used to discretize the model:

$$ X_{t+1} = X_t + \frac{T}{6}\left(\dot{X}_t + 4\dot{X}_{t,t+1} + \dot{X}_{t+1} \right) \tag{7} $$

where T is the control period. For the next time step, the following relation holds:

$$X_{t+1} = X_t + \frac{T}{6}\left(f\left(X_t, u_t\right) + 4f\left(X_{t,t+1}, u_{t,t+1}\right) + f\left(X_{t+1}, u_{t+1}\right)\right) \tag{8}$$

Here, $X(t)$ is the matrix containing all state variables, and T is the control period. Discretizing the chassis yaw angle and the manipulator joint angles over n prediction steps yields 2n discretization nodes. To reduce the computational cost, φ and q are discretized using the second-order Runge–Kutta (RK2) method.

Suppose that the robot's initial state at sampling instant t is $X = \left[x_0, y_0, \varphi_0, v_0, \delta_0, q_0, \dot{q}_0\right]$. The control sequence over a prediction horizon of \(n\) steps is expressed in matrix form as follows:

$$\begin{aligned} \hat{v}_u &= \left[v_{u1}, v_{u2}, \cdots, v_{un}\right] \\ \hat{\delta}_u &= \left[\delta_{u1}, \delta_{u2}, \cdots, \delta_{un}\right] \\ \hat{\dot{q}}_u &= \left[\dot{q}_{u1}, \dot{q}_{u2}, \cdots, \dot{q}_{un}\right] \end{aligned} \tag{9}$$

3.2 Objective Function Design

To balance the path-tracking performance of the mobile platform, the trajectory-tracking accuracy of the manipulator end effector, and the smoothness of coordinated motion, a composite objective function is formulated with tracking error terms and a control increment penalty. The control increment weighting matrix determines the penalty on changes in control inputs between consecutive control periods. The objective function is defined as follows:

$$\begin{aligned} J\left(t_k\right) = \sum_{j=1}^{N}\Big[& Q_{m,v}\left\|v_m - v_{m,ref}\right\|^2 + Q_{m,\varphi}\left\|\varphi - \varphi_m\right\|^2 + Q_{m,p}\min_j\left\|p_m - P_{m,ref}\left(j\right)\right\|^2 \\ & + Q_{ef,P}\left\|P_{ef} - P_{ef.ref}\right\|^2 + Q_{ef,v}\left\|v_{ef} - v_{ef,ref}\right\|^2\Big] + R_{uv}\left\|v_u\right\|^2 + R_{u\delta}\left\|\delta_u\right\|^2 + \sum_{j=1}^{6} R_{ui}\dot{\theta}_{ui} \end{aligned} \tag{10}$$

The objective function consists of weighted errors between the control inputs and states of the mobile platform and the manipulator end effector and their respective reference values. The reference point for the mobile platform is defined as the point on the path closest to its current position. This reference, denoted by $P_{m.ref}(t)$, is used to evaluate path-tracking performance. Path tracking by the mobile platform is independent of time. The reference trajectory sequence generated by end-effector trajectory planning is denoted by $P_{ef.ref}(t)$. The end effector follows the target trajectory at a constant speed, with $v_{ef,ref}$ denoting its reference velocity, while the mobile platform is free to move along the path. Here, $Q_{m,v}$ is the weighting coefficient for the mobile platform velocity. It determines the contribution of this velocity to the overall optimization objective and is selected according to the requirements of the coordinated task. Joint angle constraints are also imposed to account for the manipulator's range of motion and ensure that the control commands satisfy its kinematic limits.

Based on the objective function and constraints defined above, a nonlinear model predictive control optimization problem is formulated and solved to obtain the optimal control sequence over the prediction horizon:

$$u^*\left(t_k, \cdots, t_{k+N}\right) = \arg\min J(t) \tag{11}$$

Here, u^* denotes the optimal control sequence at time t_k. Only the first control input is applied to the system. At the next control cycle, the optimization is repeated using the updated state estimate.

3.3 Robot State Estimation

The NMPC formulation does not include a state estimation procedure. Sensor noise and external disturbances may therefore reduce control accuracy. An extended Kalman filter (EKF) is used to estimate the robot state. The EKF consists of the following steps.

Based on the kinematic model in Eq. (2-7), let the initial state of the mobile platform be $\left[x_{t-1} \quad y_{t-1} \quad \varphi_{t-1}\right]$. Its state at time \(t\) is then expressed as:

$$\begin{bmatrix} x_t \\ y_t \\ \varphi_t \end{bmatrix} = \begin{bmatrix} x_{t-1} + Tv_{t-1}\cos\varphi_{t-1} \\ y_{t-1} + Tv_{t-1}\sin\varphi_{t-1} \\ \varphi_{t-1} + Tv_{t-1}\tan\delta_{t-1}/l \end{bmatrix} \tag{12}$$

With sensor noise included, the state-space equation is given by:

$$\begin{bmatrix} x_t \\ y_t \\ z_t \end{bmatrix} = \begin{bmatrix} 1 & 0 & -Tv_{t-1}\sin\varphi_{t-1} \\ 0 & 1 & Tv_{t-1}\cos\varphi_{t-1} \\ 0 & 0 & 1 \end{bmatrix} \begin{bmatrix} x_{t-1} \\ y_{t-1} \\ z_{t-1} \end{bmatrix} + \begin{bmatrix} T\cos\varphi_{t-1} & 0 \\ T\sin\varphi_{t-1} & 0 \\ \frac{T}{l}\tan\delta_{t-1} & \frac{Tv_{t-1}}{l\cos^2\delta_{t-1}} \end{bmatrix} \begin{bmatrix} v_{t-1} \\ \delta_{t-1} \end{bmatrix} + Noise \tag{13}$$

In the experiments presented later, an EKF is used to estimate the pose of the mobile platform. Its effectiveness is evaluated by comparing the estimated and measured poses with the reference pose and analyzing the corresponding tracking errors.

4. Experimental Results and Analysis

4.1 Simulation Setup and Parameter Configuration

The simulation model is based on the physical parameters of the actual robot platform. The robot is first modeled in SolidWorks, where the coordinate transformations between the chassis and the manipulator, as well as those between the manipulator joints, are defined. The model is then exported as a Unified Robot Description Format (URDF) file and imported into CoppeliaSim. After further configuration, the simulation environment shown in Figure 3 is obtained.

CoppeliaSim executes motion commands and provides real-time operating data. The control module in Simulink performs path planning, trajectory planning, and coordinated control. Communication between CoppeliaSim and Simulink is implemented using a dedicated interface library. The simulation sampling period is set to 100 ms.

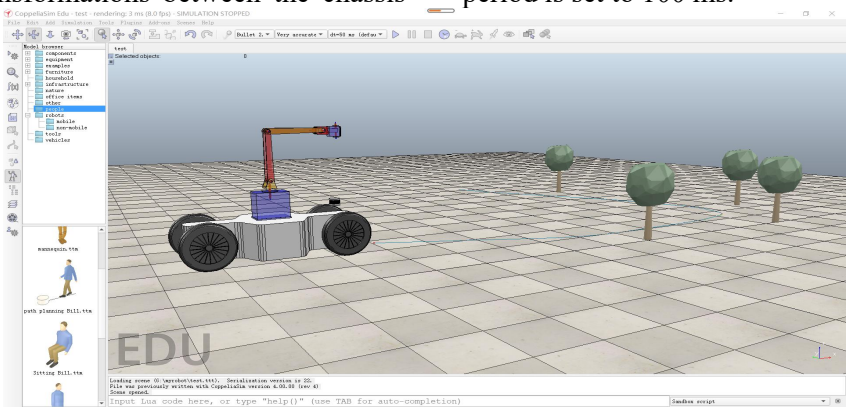
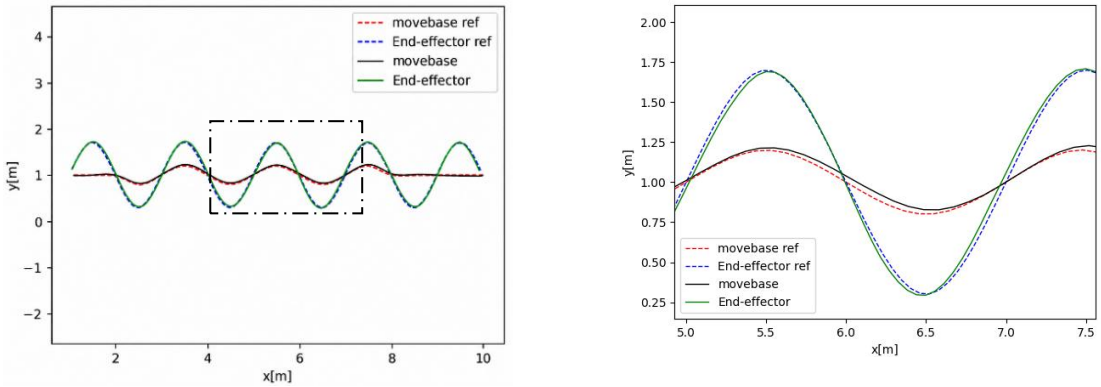


Figure 3. Simulation Model of the Mobile Robot

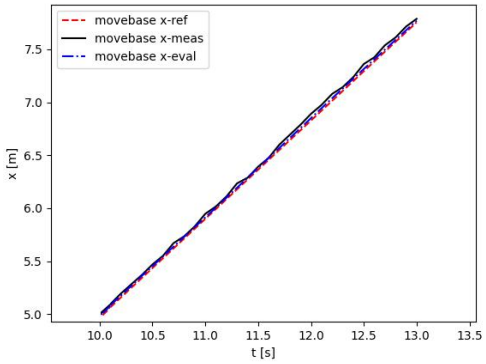
4.2 Simulation Tests

Simulation tests are conducted using the model described in the previous section to verify that the proposed controller can coordinate the mobile platform and the manipulator. The target path for the mobile platform consists of two straight segments and a sinusoidal curve, with a total length of approximately 10.5 m. The target trajectory for the manipulator end effector is a sinusoidal curve with an amplitude of 0.8 m and a wavelength of 2 m. The paths are shown in Figure 4. The coordinated controller operates at 10 Hz, with a prediction horizon of 100 integration steps.

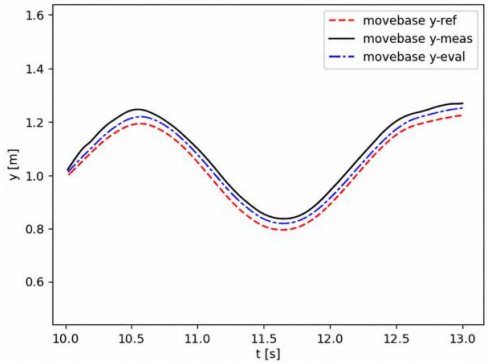


(a) Simulation Paths (b) Enlarged View

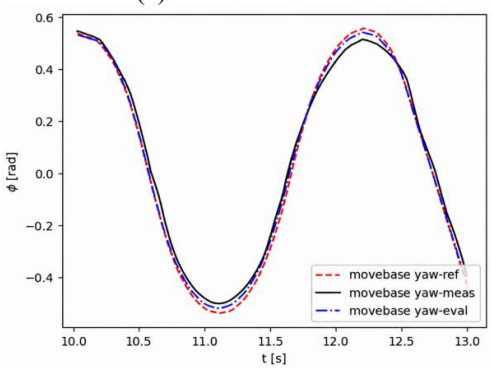
Figure 4. Trajectory Tracking in Simulation



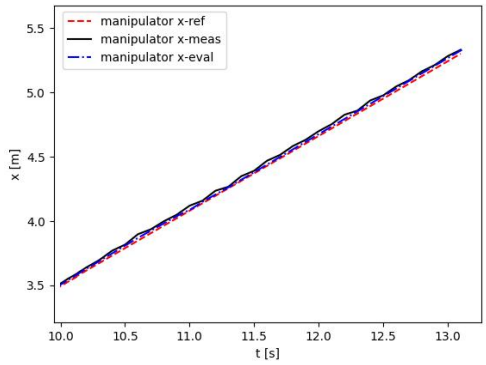
(a) X of Movebase



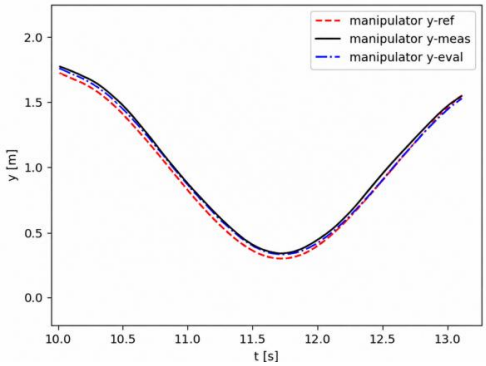
(b) y of Movebase



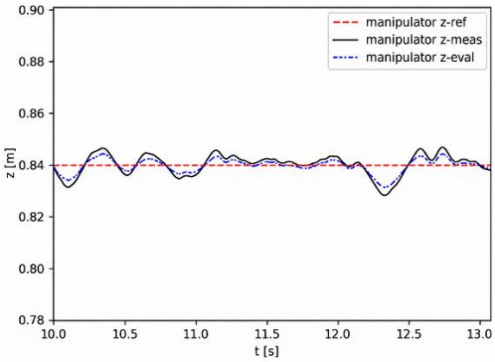
(c) φ of Movebase



(d) x of Manipulator



(e) y of Manipulator



(f) z of Manipulator

Figure 5. Time Histories of the Mobile Platform Pose and End-Effector Position

In the simulation with the end-effector speed set to 1.0 m/s, data from 10 to 13 s are selected for analysis. The reference, measured, and estimated values of the observed variables are shown in Figure 5. Panels (a)–(c) show the time histories of the mobile platform's x, y, and φ, respectively. Panels (d)–(f) show the time histories of the end effector's x, y, and z coordinates, respectively.

To evaluate the controller's stability, the tracking errors of the mobile platform and the manipulator end effector are measured at end-effector speeds of 0.5m/s, 1.0m/s, and 1.5 m/s. Box plots of the tracking errors are shown in Figure 6.

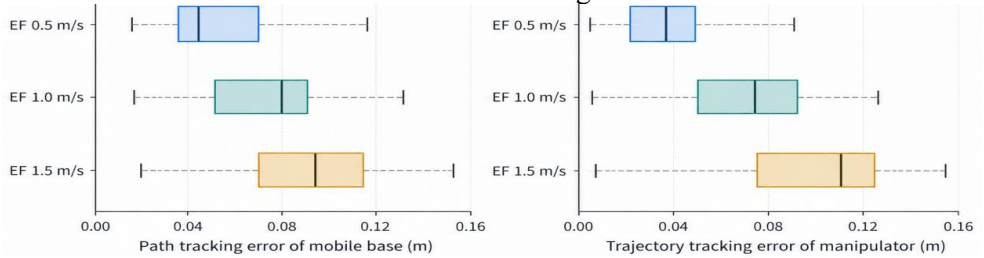


Figure 6. Tracking Errors of the Mobile Platform and Manipulator at end-Effector Speeds of 0.5, 1.0, and 1.5 m/s

The tracking errors of the mobile platform and the manipulator end effector are used to evaluate the performance of coordinated control. The platform's path-tracking error is defined as the Euclidean distance between its measured position and the nearest point on the reference path. The end-effector trajectory-tracking error is defined as the Euclidean distance between its actual position and the reference trajectory point at the corresponding time. Across the tested end-effector speeds, the mean path-tracking error of the mobile platform ranges from 4.63 to 14.87 cm, while the mean trajectory-tracking error of the end effector ranges from 4.18 to 12.53 cm. The platform's path-tracking error generally increases with end-effector speed, indicating that faster manipulator motion affects coordinated tracking performance. Overall, both tracking errors remain within the allowable limits specified for the experiments, demonstrating that the proposed control method can coordinate the motion of the mobile platform and the manipulator.

The reference states, measured states, and EKF estimates of the mobile platform are also compared. The EKF estimates show smaller deviations from the reference states than the direct measurements, suggesting that the EKF can improve state estimation accuracy to some extent. However, temporal offsets are observed among the estimated, measured, and reference values. These offsets may be related to the state prediction horizon, data acquisition, and time synchronization within the control system. Since the controller uses predicted states for receding-horizon optimization, the temporal alignment between these states and the reference trajectory directly affects the evaluation of tracking errors. As the end-effector speed increases, the system requires more accurate state estimates and faster control responses, while the robot's overall tracking accuracy decreases.

The end-effector pose is expressed in the world coordinate frame, and the manipulator inverse kinematics are solved using the mobile platform pose estimated by the EKF. The end-effector tracking error must therefore be calculated in this common world frame. The platform's path-tracking error and the end-effector tracking error should not be added directly. However, errors in the estimated platform pose affect the end effector's actual positioning accuracy through coordinate transformations and inverse kinematics. End-effector trajectory-tracking performance thus depends on the manipulator's motion control accuracy, the accuracy of the platform pose estimates, and the coordinated control strategy.

5. Conclusions

This paper proposes a coordinated control method for a mobile manipulator. The method allows the end effector to follow its target trajectory while the mobile platform moves independently along a collision-free path. It relaxes the restrictions imposed by conventional coordinated control algorithms on path geometry and platform holonomic constraints, offering broader applicability.

Simulation tests demonstrate that the end effector and the mobile platform can simultaneously track their respective trajectory and path. The overall tracking accuracy meets the requirements of low-speed operations, although accuracy decreases as the operating speed increases. Future work will investigate feedforward compensation for the platform pose to reduce the effects of pose estimation delay. The simulation results confirm the effectiveness of the proposed NMPC-based coordinated control method and support its application to low-speed mobile manipulation tasks in agriculture, warehousing, and logistics.

Acknowledgments

This paper is supported by the General Institutional Natural Science Research Project of Chongqing Industry & Trade Polytechnic (No. ZR202433).

References

[1] Lu Z, Wang Y. A differentiable dynamic modeling approach to integrated motion planning and actuator physical design for mobile manipulators. Journal of Field Robotics, 2025, 42(1): 37–64.

[2] Gao S, Zhu Y, et al. Motion-force control of mobile manipulators via extended uncertainty and disturbance estimation. Control Engineering Practice, 2026, 167: 106650.

[3] Sun P Y, Li J, Liu Y F, et. al. Compliant Door-opening Technology for Mobile Manipulator Based on Platform-manipulator Collaboration Strategy. Robot, 2026, 48(1): 102-115.

[4] Wu C, Wang R, Song M, et al. Real-time

whole-body motion planning for mobile manipulators using environment-adaptive search and spatial-temporal optimization. IEEE International Conference on Robotics and Automation. 2024.

[5] Qin D, Wu J, Liu A, et al. Cooperation and coordination transportation for nonholonomic mobile manipulators: A distributed model predictive control approach. IEEE Transactions on Systems, Man, and Cybernetics: Systems, 2023, 53(2): 848–860.

[6] Du X T, Zhou S Q, Schoellig AP. Hierarchical task model predictive control for sequential mobile manipulation tasks. IEEE Robotics and Automation Letters, 2024, 9(2): 1270–1277.

[7] Geng M. Research on Mobile Grasping Problem of Composite Robot Based on Hierarchical Cooperative Control. Yanshan University, 2025.

[8] Liu C, Qin T. Motion control of four-wheel distributed drive mobile robot based on MPC, 2025, (5): 6-12.

[9] Kashi Z, Yadegar M, Meskin N, et al. Safe model predictive control of a non-holonomic mobile manipulator under multiple constraints using control barrier functions. IEEE Access, 2025, 13: 76638–76653.

[10] Liu S, Wang F, Li B L. Simulation of Robot Trajectory Tracking Control under Nonholonomic Constraints. Computer Simulation, 2023, 40(10): 422-425+444.

[11] Wang Y, Chen R, Zhao M. Whole-body model predictive control for mobile manipulation with task priority transition. IEEE International Conference on Robotics and Automation. 2025.

[12] Shen W, Hu Y, Liu Y, et al. Holistic model predictive control for mobile manipulation. IEEE International Conference on Automation Science and Engineering. 2026.